

## Isospin effect of fragmentation reactions induced by intermediate energy heavy ions and its disappearance

D. Q. Fang,<sup>2</sup> W. Q. Shen,<sup>1,2,\*</sup> J. Feng,<sup>2</sup> X. Z. Cai,<sup>2</sup> J. S. Wang,<sup>2</sup> Q. M. Su,<sup>2</sup> Y. G. Ma,<sup>1,2</sup> Y. T. Zhu,<sup>3</sup> S. L. Li,<sup>3</sup> H. Y. Wu,<sup>3</sup>  
Q. B. Gou,<sup>3</sup> G. M. Jin,<sup>3</sup> W. L. Zhan,<sup>3</sup> Z. Y. Guo,<sup>3</sup> and G. Q. Xiao<sup>3</sup>

<sup>1</sup>CCAST (World Laboratory) P.O. Box 8730, Beijing, 100080, China

<sup>2</sup>Shanghai Institute of Nuclear Research, Chinese Academy of Sciences, Shanghai 201800, China

<sup>3</sup>Institute of Modern Physics, Chinese Academy of Sciences, Lanzhou 730000, China

(Received 3 September 1999; published 21 March 2000)

The fragments produced in the reaction of  $^{18}\text{O}+^9\text{Be}$  at 60 MeV/nucleon were measured experimentally. The isotopic distribution of the fragmentation reaction products was well reproduced by using a modified statistical abrasion-ablation model. This model predicts that the fragment isotopic distribution at a fixed atomic number  $Z$  shifts towards the neutron rich side for the neutron-rich projectile. This isospin effect will decrease with decreasing the fragment atomic number  $Z$  and disappear when  $(Z_{\text{proj}}-Z)/Z_{\text{proj}}$  becomes larger than 0.5. It was shown that the disappearance of the isospin effect of fragmentation reaction is induced by the geometry effect in abrasion stage and the evaporation effect later.

PACS number(s): 25.70.Mn, 24.10.Pa

Recently the development of the radioactive ion beam (RIB) technique has stimulated the research of the nuclear reaction induced by exotic nuclei both experimentally and theoretically. The studies using RIB demonstrated that a large enhancement of the total reaction cross section  $\sigma_R$  induced by neutron-rich nuclei was found in some experiments which was interpreted as neutron halo (such as  $^{11}\text{Li}$ ,  $^{11,14}\text{Be}$ ,  $^{19}\text{C}$ , etc.) and neutron skin (such as  $^6\text{He}$  and  $^8\text{He}$ ) structure [1–4]. The discovery of these unusual phenomena evokes further theoretical and experimental research on proton halo and proton skin, e.g., whether  $^8\text{B}$  has proton halo or not has been investigated extensively [3,5,6]. The most important experimental base of this research is the production of RIB with high intensity and good quality. In the past decades, the projectile fragmentation (PF) reaction has proved to be one of the very efficient ways to produce RIB. The characteristics of PF reaction have been researched in detail, while the exotic nuclei used to measure  $\sigma_R$  are almost produced by PF method. The investigation of the fragment isotopic distribution in the fragmentation reaction induced by heavy ions at intermediate energies can provide not only a valuable insight into the reaction mechanism but also a good reference for producing neutron- or proton-rich exotic nuclei. The study of the characteristic of nuclear reaction by using RIB, e.g., isospin effect on nuclear reaction, etc., also has great significance. In this paper, we present the experimental measurement of the fragment isotopic distribution in the fragmentation reaction of  $^{18}\text{O}+^9\text{Be}$  at 60 MeV/nucleon. Comparison with a modified statistical abrasion-ablation model calculation was made. Isospin effect and its disappearance for the fragment isotopic distribution in a fragmentation reaction are also discussed within the framework of this model.

The experiment was performed at the Radioactive Ion Beam Line in Lanzhou (RIBLL) using a beam of 60 MeV/nucleon  $^{18}\text{O}$  delivered by the Heavy Ion Research Facility in

Lanzhou (HIRFL) bombarding on a Be (370 mg/cm<sup>2</sup>) target. After the first focal plane RIBLL can be used as a magnetic spectrometer. The target was mounted at the first focal plane of RIBLL where nuclei produced in the reaction were selected and collected. The angular acceptance was 6.5 msr, and the fragments emitted between  $-2.61^\circ$  and  $2.61^\circ$  could be transmitted through the spectrometer. Since the projectile fragments are strongly focused around  $0^\circ$ , the good collection is obtained in a cone around these angles. The momentum acceptance  $\Delta P/P$  of the magnetic spectrometer was set at about 10%. The time of flight (TOF) of the fragments was measured by two scintillator detectors with a flight path of 16.8 m. A telescope consisting of three transmission Si surface barrier detectors and one CsI(Tl) crystal gave the energy losses ( $\Delta E$ ) and total energy ( $E$ ) of the reaction products, respectively [7,8]. Combining TOF and  $\Delta E$  makes it possible to identify the reaction products and get the production yields of the fragments directly [7,8].

The experimental results were compared with the statistical abrasion-ablation model developed by Brohm *et al.* [9] which considers the independent nucleon-nucleon collisions in the overlap zone of the colliding nuclei to determine the distributions of abraded neutrons and protons. This model is quite successful in describing the fragmentation reaction at high energies. However, some modification is required in order to describe the nuclear collision of neutron-rich nuclei at intermediate energies due to the medium effect of nucleon-nucleon collision and the larger neutron density distribution radii for a neutron-rich nucleus. In a heavy ion reaction at intermediate energies, the in-medium nucleon-nucleon collision cross section is different from the free nucleon-nucleon collision cross section due to the influence of the nuclear density distribution. In our calculation we have used the in-medium nucleon-nucleon collision cross section proposed by our group given in Ref. [10].

The nuclear surface distribution has great effect on the nucleon-nucleon interaction in the reaction. For stable nuclei the diffuseness is around 2.4 fm, which is predicted by the droplet model due to a nearly constant nuclear separation energy (about 8 MeV/nucleon). For exotic nuclei the loosely

\*Corresponding author.

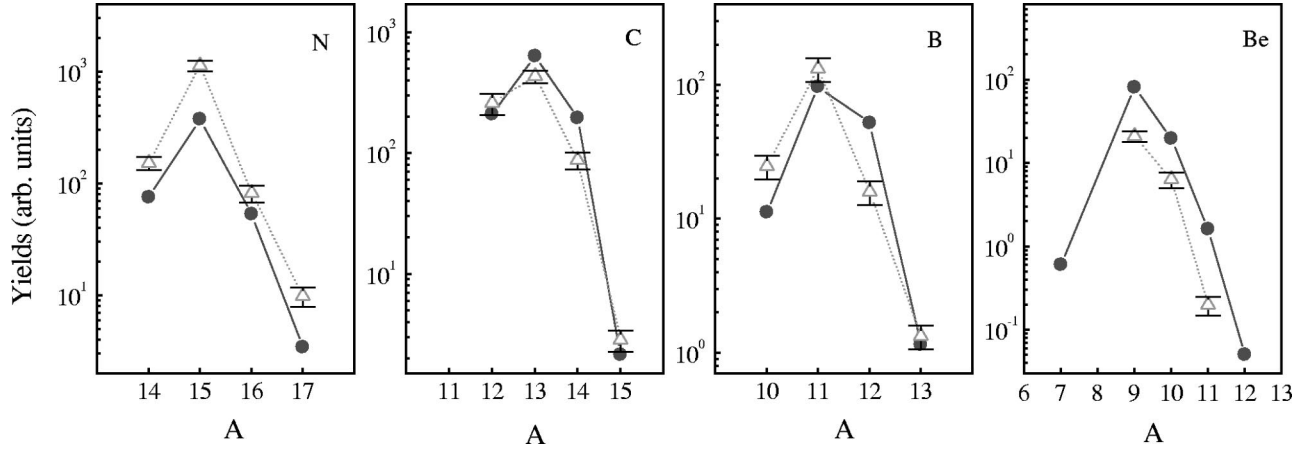


FIG. 1. The fragment isotopic distribution produced by 60 MeV/nucleon  $^{18}\text{O}$  on Be. The dots are calculated by the model, the triangles are the experimental results. Statistical error bars are shown for the experimental results.

bound nucleons with small separation energy will cause a long tail in the nucleon distribution. Considering these results, we use the diffuseness parameter  $t_N$  for neutron distribution as a function of neutron separation energy  $\varepsilon$  (in units of MeV) given in Ref. [11].

These modifications make this model applicable to fragmentation reaction involving neutron or proton rich nuclei over a wide energy range. It was shown that this modified model could reproduce the isotopic distributions of the fragments in 44 MeV/nucleon  $^{40}\text{Ar}$ ,  $^{86}\text{Kr}$ , and  $^{129}\text{Xe}$  induced fragmentation reactions [12].

In Fig. 1 a comparison is made for the fragment isotopic distribution in the fragmentation reaction induced by 60 MeV/nucleon  $^{18}\text{O}$  on Be with the modified statistical abrasion-ablation model calculation results. The peak positions of the fragment isotopic distribution are well reproduced by using the model, and the agreement of the shapes of the fragment isotopic distribution between experiment and calculation is also satisfactory. The angular and magnetic rigidity acceptances of the spectrometer were considered in the above calculations in order to get yields directly comparable to the experimental data. The angular and momentum distributions of the fragments were calculated according to Durand's model [13]. Then the momentum distribution was transformed into magnetic rigidity distribution. From the angular and magnetic rigidity distributions two reduced factors

could be obtained for every fragment according to the limited acceptances of angular and magnetic rigidity of the spectrometer in the experiment. Then the fragment production cross section calculated by the modified statistical abrasion-ablation model was multiplied by these two factors for every fragment.

For the production of nuclei far from the  $\beta$ -stability line, the isospin effect of fragmentation reaction on the isotopic distribution is a very interesting topic. The fragment isotopic distributions in the fragmentation reaction induced by 60 MeV/nucleon  $^{16}\text{O}$  and  $^{18}\text{O}$ ,  $^{36}\text{Ar}$  and  $^{40}\text{Ar}$ ,  $^{40}\text{Ca}$  and  $^{48}\text{Ca}$  are compared through the modified statistical abrasion-ablation model calculation [8]. Figure 2 shows the results for  $^{36}\text{Ar}$  and  $^{40}\text{Ar}$  bombardment. It is demonstrated that the isotopic distribution of fragmentation reaction products shifts toward the neutron-rich side for a neutron-rich projectile, but this isospin effect decreases with the increase of the atomic number difference  $Z_{\text{proj}}-Z$ , where  $Z_{\text{proj}}$  is the projectile atomic number, and disappears at last.

In order to understand the isospin effect of the fragmentation reaction on the isotopic distribution more clearly, the peak positions and widths were extracted by a Gaussian fit to the fragment isotopic distributions. The difference  $\Delta A = A_{\text{peak}} - A_{\beta}$ , which describes the peak position relative to most  $\beta$ -stable mass and width of the isotopic distribution as a function of  $(Z_{\text{proj}}-Z)/Z_{\text{proj}}$ , were given in Fig. 3, where

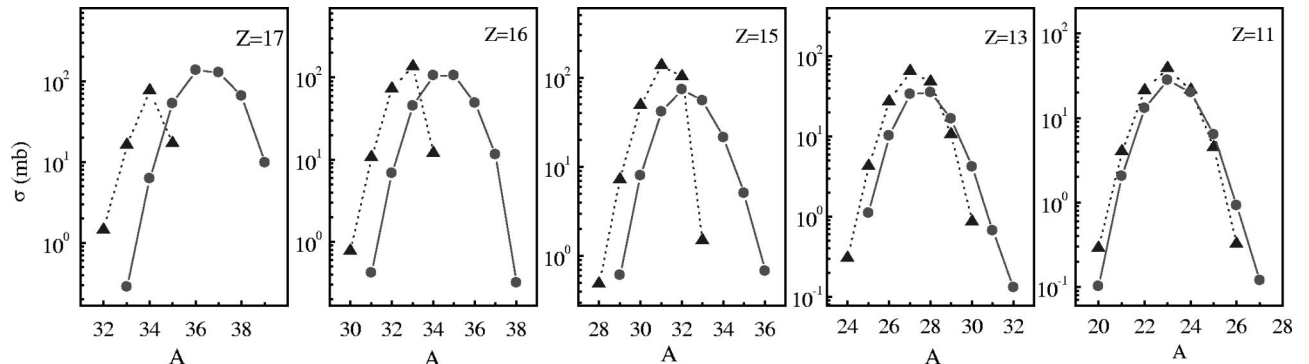


FIG. 2. Comparison of the fragment isotopic distribution produced by 60 MeV/nucleon  $^{40}\text{Ar}$  (dots) and  $^{36}\text{Ar}$  (triangles) on Be.

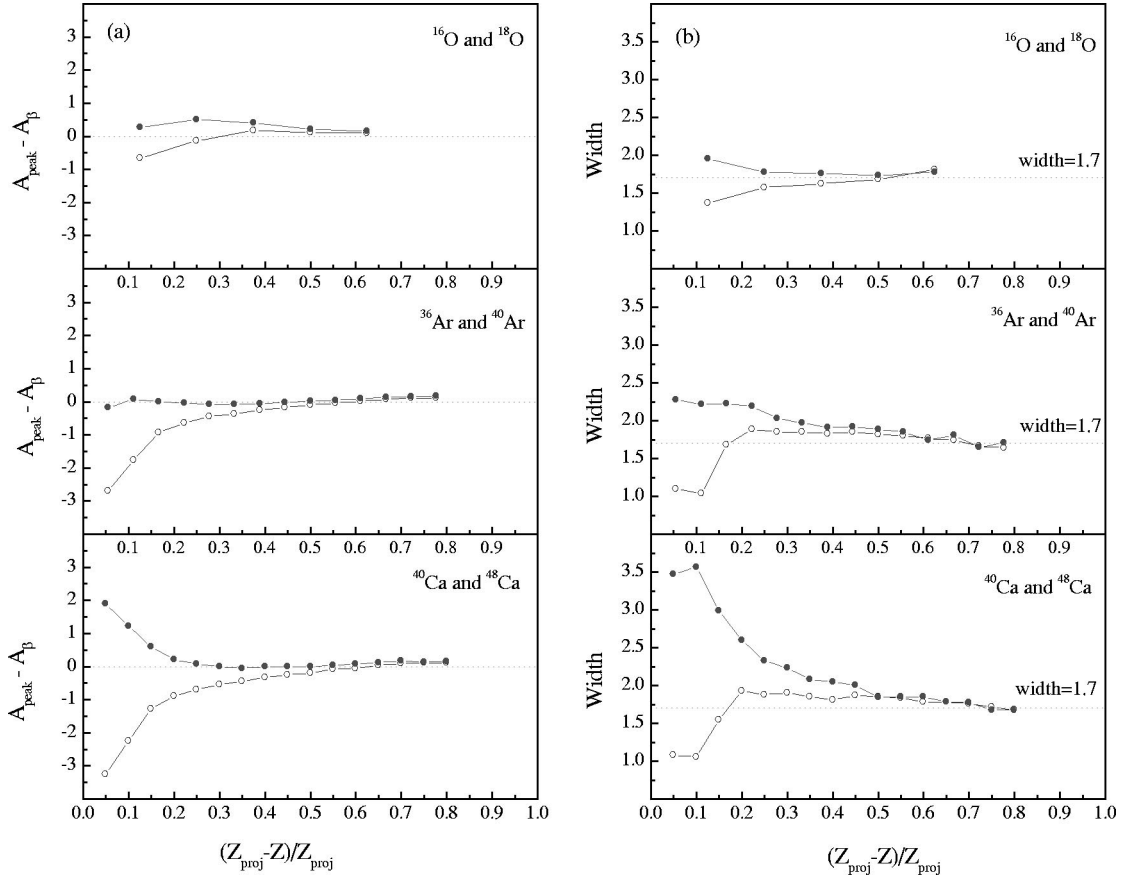


FIG. 3. The difference  $A_{\text{peak}} - A_{\beta}$  (a) and width (b) of the fragment isotopic distribution as a function of  $(Z_{\text{proj}} - Z)/Z_{\text{proj}}$ . The solid circles are the results of the neutron-rich projectiles  $^{18}\text{O}$ ,  $^{40}\text{Ar}$ , and  $^{48}\text{Ca}$ . The open circles are the results of  $^{16}\text{O}$ ,  $^{36}\text{Ar}$ , and  $^{40}\text{Ca}$ .

$A_{\text{peak}}$  is peak position of the fragment isotopic distribution,  $A_{\beta}$  is the mass of most  $\beta$ -stable nucleus of the isotope determined by  $Z = A_{\beta} / (1.98 + 0.0155 * A_{\beta}^{2/3})$  [14]. Roughly speaking, the parameter  $(Z_{\text{proj}} - Z)/Z_{\text{proj}}$  can be viewed as the violence of the nuclear reaction which is related to the reaction time, the dissipated energy or the excitation energy and the impact parameter. From Fig. 3 we can see that  $\Delta A$  becomes larger for a more neutron-rich projectile, but it approaches zero when  $(Z_{\text{proj}} - Z)/Z_{\text{proj}}$  comes close to 0.5 and becomes approximately zero for  $(Z_{\text{proj}} - Z)/Z_{\text{proj}}$  larger than 0.5 for the three reaction systems mentioned above. The width of the fragment isotopic distribution also becomes larger for a more neutron-rich projectile and approaches a constant value around 1.7 when  $(Z_{\text{proj}} - Z)/Z_{\text{proj}}$  is larger than 0.5 for these three reaction systems. This demonstrates that the isospin effect of the projectile fragmentation reaction on the isotopic distribution becomes smaller with the increase of  $(Z_{\text{proj}} - Z)/Z_{\text{proj}}$  or the violence of the nuclear reaction. The fragment isotopic distributions produced by different projectiles show little difference for  $(Z_{\text{proj}} - Z)/Z_{\text{proj}}$  larger than 0.5, i.e., the isospin effect of the projectile fragmentation on the isotopic distribution at a fixed atomic number  $Z$  will disappear under the above condition.

In the statistical abrasion-ablation model, the nuclear reaction is described in two stages which occur in two distinctly different time scales. The first abrasion stage is fragmentation reaction which describes the production of the

prefragment with certain amount of excitation energy through the nucleon-nucleon collision in the overlap zone of the projectile and target. In the second evaporation stage the system reorganizes, which means it deexcites and thermalizes by the evaporation of particles. In order to explain the disappearance of the isospin effect, the normalized peak position difference  $\Delta A_{\text{peak}} / \Delta A_{\text{proj}}$  of the fragment isotopic distribution before and after the evaporation as a function of  $(Z_{\text{proj}} - Z)/Z_{\text{proj}}$  was given in Fig. 4, where  $\Delta A_{\text{proj}}$  is the mass number difference of two projectiles with the same charge number  $Z$  and  $\Delta A_{\text{peak}}$  is the peak position difference of the fragmentation isotopic distribution produced by different projectiles. It can be seen from the figure that  $\Delta A_{\text{peak}} / \Delta A_{\text{proj}}$  after evaporation will decrease and become zero at last with the increase of  $(Z_{\text{proj}} - Z)/Z_{\text{proj}}$ . This is the result of the disappearance of the isospin effect. At the same time the decrease of  $\Delta A_{\text{peak}} / \Delta A_{\text{proj}}$  before evaporation with the increase of  $(Z_{\text{proj}} - Z)/Z_{\text{proj}}$  indicates that the isospin effect is also decreasing with the increase of  $(Z_{\text{proj}} - Z)/Z_{\text{proj}}$  in abrasion stage. This exhibits that the geometry effect in abrasion stage and the evaporation will lead to the decrease of the isospin effect with the increase of  $(Z_{\text{proj}} - Z)/Z_{\text{proj}}$ . These phenomena may be explained as follows. For peripheral reaction, it is dominated by the nucleon-nucleon interaction of the nuclear surface where nucleons are loosely bound and the neutron and proton density distribution is quite different for neutron rich nuclei. This makes the isospin effect exhibit in the frag-

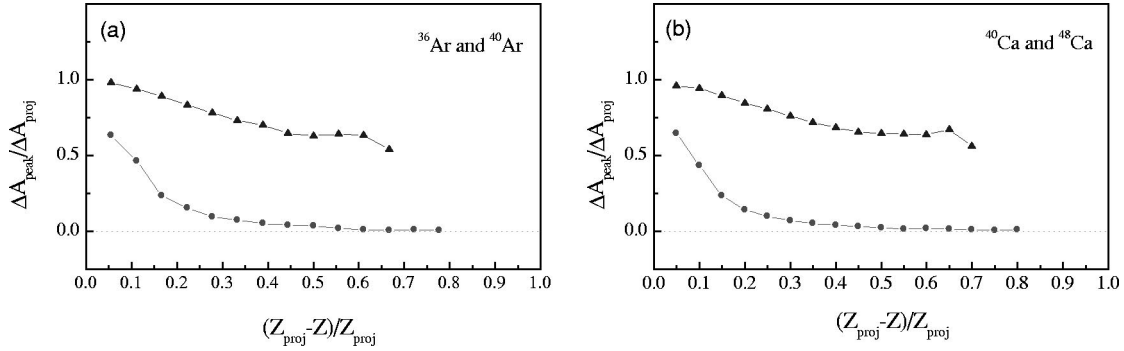


FIG. 4. The normalized peak position difference  $\Delta A_{\text{peak}}/\Delta A_{\text{proj}}$  of the fragment isotopic distribution produced by  $^{40}\text{Ar}$  and  $^{36}\text{Ar}$  (a),  $^{48}\text{Ca}$  and  $^{40}\text{Ca}$  (b) as a function of  $(Z_{\text{proj}}-Z)/Z_{\text{proj}}$ . The dots are the result after evaporation and the triangles are the result before evaporation.

ment isotopic distribution. With increasing  $Z_{\text{proj}}-Z$ , roughly speaking, the impact parameter is decreasing. For a more central reaction, it is dominated by the nucleon-nucleon interaction of the more central part of the nucleon distribution where nucleons are closely bound and the neutron and proton density distribution have little difference. At the same time, the excitation energy of the prefragment would be higher for a more central reaction and it is easier for more neutron-rich nuclei to evaporate more neutrons. So the isospin effect will be washed out further by the sequential evaporation process. This may be the reason that the isospin effect of the fragment isotopic distribution disappears for  $(Z_{\text{proj}}-Z)/Z_{\text{proj}}$  larger than 0.5.

These results may be helpful for choosing a suitable projectile to produce the expected neutron-rich exotic nuclei with RIB. It is better to use a neutron-rich projectile with an atomic number not far away from the expected exotic nuclei because the difference in the fragmentation cross sections induced by neutron-rich and stable projectiles became small with the increase of  $Z_{\text{proj}}-Z$ . But it should be pointed out that the reaction mechanism of the production of exotic nuclei in intermediate energy heavy ion collisions is very complicated. Multinucleon transfer and multifragmentation reaction could produce exotic nuclei besides projectile fragmentation reaction. The fragment with mass and charge number far from that of the projectile may be produced mainly by a multifragmentation reaction that has a strong isospin effect at intermediate energies and makes the neutron-rich projectile have a quite large production cross section of neutron-rich exotic nuclei.

Recently Miller *et al.* [15] have found the disappearance of the isospin effect of the multifragmentation when the incident energy changes from low energy to the high energy. It has some similarity to the isospin effect of the fragmentation reaction discussed here except with a different disappearance

condition. In the past years, the isospin dependence of various physical quantities has been reported [16–21]. The studies show that the isospin effect exists in the nuclear reaction induced by exotic nuclei but it may disappear under certain condition. This makes us believe that the isospin effect of some physical quantity such as multifragmentation flow, and isotopic distribution, etc., and its disappearance may be a common phenomenon of RIB induced nuclear reaction.

In summary, we have measured the fragment isotopic distribution for 60 MeV/nucleon  $^{18}\text{O}$  on Be experimentally. A way to fit the experimental isotopic distribution with a modified statistical abrasion-ablation model is developed based on Durand's model calculation for angular and momentum distributions of fragments. The isotopic distribution of the fragmentation reaction products was well reproduced by the modified statistical abrasion-ablation model via this method. The isospin effect of the fragmentation reaction on the fragment isotopic distribution was investigated within this model. The fragment isotopic distribution shifts toward the neutron-rich side for a neutron-rich projectile, but the shift decreases with the increase of the atomic number difference  $Z_{\text{proj}}-Z$  or the violence of the nuclear reaction. The isospin effect of the fragmentation reaction on the fragment isotopic distribution will disappear when  $(Z_{\text{proj}}-Z)/Z_{\text{proj}}$  becomes larger than 0.5. It has been shown that the disappearance of isospin effect is the result of the geometry effect in the abrasion stage and the sequential evaporation process.

We would like to thank the members of the RIBLL group and the HIRFL staff members for all their help and the nice  $^{18}\text{O}$  beam. This work was supported by the National Science Foundation of China for Distinguished Young Scholars under Grant No. 19625513, the National Science Foundation of China under Grant No. 19675059, Shanghai Science and Technology Development Fund under Grant No. 96XD14011.

- [1] I. Tanihata, H. Hamagaki, O. Hashimoto, Y. Shida, N. Yoshikawa, K. Sugimoto, O. Yamakawa, T. Kobayashi, and N. Takahashi, Phys. Rev. Lett. **55**, 2676 (1985).  
 [2] I. Tanihata, H. Hamagaki, O. Hashimoto, Y. Shida, N. Yoshikawa, K. Sugimoto, O. Yamakawa, T. Kobayashi, and

T. Takahashi, Phys. Lett. **160B**, 380 (1985).

- [3] I. Tanihata, T. Kobayashi, O. Yamakawa, S. Shimoura, K. Ekuni, K. Sugimoto, T. Takahashi, T. Shimoda, and H. Sato, Phys. Lett. B **206**, 592 (1988).  
 [4] I. Tanihata, T. Kobayashi, T. Suzuki, Y. Yoshida, S. Shi-

- moura, K. Sugimoto, K. Matsuta, T. Minamisono, W. Christie, D. Olson, and H. Wieman, *Phys. Lett. B* **287**, 307 (1992).
- [5] B. Blank, C. Marchand, M. S. Pravikoff, T. Baumann, F. Boue, H. Geissel, M. Hellstrom, N. Iwasa, W. Schwab, K. Summerer, and M. Gai, *Nucl. Phys.* **A624**, 242 (1997).
- [6] F. Negoita, C. Borcea, F. Carstoiu, M. Lewitowicz, M. G. Saint-Laurent, R. Anne, D. Bazin, J. M. Corre, P. Roussel-Chomaz, V. Borrel, D. Guillemaud-Mueller, H. Keller, A. C. Mueller, F. Pougheon, O. Sorlin, S. Lukyanov, Yu. Penionzhkevich, A. Fomichev, N. Skobelev, O. Tarasov, Z. Dlouhy, and A. Kordyasz, *Phys. Rev. C* **54**, 1787 (1996).
- [7] D. Q. Fang, J. Feng, X. Z. Cai, J. S. Wang, W. Q. Shen, Y. G. Ma, Y. T. Zhu, S. L. Li, H. Y. Wu, Q. B. Gou, G. M. Jin, W. L. Zhan, Z. Y. Guo, and G. Q. Xiao, *Chin. Phys. Lett.* **16**, 15 (1999).
- [8] D. Q. Fang, W. Q. Shen, J. Feng, X. Z. Cai, J. S. Wang, Q. M. Su, Y. G. Ma, Y. T. Zhu, S. L. Li, H. Y. Wu, Q. B. Gou, G. M. Jin, W. L. Zhan, Z. Y. Guo, and G. Q. Xiao, *Chin. Phys. Lett.* (to be published).
- [9] T. Brohm and K. H. Schmidt, *Nucl. Phys.* **A569**, 821 (1994).
- [10] X. Z. Cai, J. Feng, W. Q. Shen, Y. G. Ma, J. S. Wang, and W. Ye, *Phys. Rev. C* **58**, 572 (1998).
- [11] J. Feng, W. Q. Shen, and Y. G. Ma, *Phys. Lett. B* **305**, 9 (1993).
- [12] D. Q. Fang, J. Feng, W. Q. Shen, X. Z. Cai, J. S. Wang, W. Ye, and Y. G. Ma, *High Energy Phys. Nucl. Phys.* **23**, 475 (1999).
- [13] D. Durand, *Nucl. Phys.* **A541**, 266 (1992).
- [14] K. Summerer, W. Bruchle, D. J. Morrissey, M. Schadel, B. Schweryn, and Yang Weifan, *Phys. Rev. C* **42**, 2546 (1990).
- [15] M. L. Miller, O. Bjarki, D. J. Magestro, R. Pak, N. T. B. Stone, M. B. Tonjes, A. M. Vander Molen, G. D. Westfall, and W. A. Friedman, *Phys. Rev. Lett.* **82**, 1399 (1999).
- [16] J. F. Dempsey, R. J. Charity, L. G. Sobotka, G. J. Kunde, S. Gaff, C. K. Gelbke, T. Glasmacher, M. J. Huang, R. C. Lemmon, W. G. Lynch, L. Manduci, L. Martin, M. B. Tsang, D. K. Agnihotri, B. Djerroud, W. U. Schroder, W. Skulski, J. Toke, and W. A. Friedman, *Phys. Rev. C* **54**, 1710 (1996).
- [17] B. A. Li, Z. Ren, C. M. Ko, and S. J. Yennello, *Phys. Rev. Lett.* **76**, 4492 (1996).
- [18] R. Pak, W. Benenson, O. Bjarki, J. A. Brown, S. A. Hannuschke, R. A. Lacey, B. A. Li, A. Nadasen, E. Norbeck, P. Pogodin, D. E. Russ, M. Steiner, N. T. B. Stone, A. M. Vander Molen, G. D. Westfall, L. B. Yang, and S. J. Yennello, *Phys. Rev. Lett.* **78**, 1022 (1997).
- [19] R. Pak, B. A. Li, W. Benenson, O. Bjarki, J. A. Brown, S. A. Hannuschke, R. A. Lacey, D. J. Magestro, A. Nadasen, E. Norbeck, D. E. Russ, M. Steiner, N. T. B. Stone, A. M. Vander Molen, G. D. Westfall, L. B. Yang, and S. J. Yennello, *Phys. Rev. Lett.* **78**, 1026 (1997).
- [20] L. W. Chen, F. S. Zhang, and G. M. Jin, *Phys. Rev. C* **58**, 2283 (1998).
- [21] S. Kumar, M. K. Sharma, R. K. Prui, K. P. Singh, and I. M. Govil, *Phys. Rev. C* **58**, 3494 (1998).